Lack of Type VIII Collagen in Mice Ameliorates Diabetic Nephropathy

Ulrike Hopfer,[1] Helmut Hopfer,[2] Catherine Meyer-Schwesinger,[1] Ivonne Loeffler,[3] Naomi Fukai,[4] Bjorn R. Olsen,[4] Rolf A.K. Stahl,[1] and Gunter Wolf[3]

OBJECTIVE—Key features of diabetic nephropathy include the accumulation of extracellular matrix proteins. In recent studies, increased expression of type VIII collagen in the glomeruli and tubulointerstitium of diabetic kidneys has been noted. The objectives of this study were to assess whether type VIII collagen affects the development of diabetic nephropathy and to determine type VIII collagen–dependent pathways in diabetic nephropathy in the mouse model of streptozotocin (STZ)-induced diabetes.

RESEARCH DESIGN AND METHODS—Diabetes was induced by STZ injections in collagen VIII–deficient or wild-type mice. Functional and histological analyses were performed 40 days after induction of diabetes. Type VIII collagen expression was assessed by Northern blots, immunohistochemistry, and real-time PCR. Proliferation of primary mesangial cells was measured by thymidine incorporation and direct cell counting. Expression of phosphorylated extracellular signal–regulated kinase (ERK1/2) and $p27^{Kip1}$ was assessed by Western blots. Finally, *Col8a1* was stably overexpressed in mesangial cells.

RESULTS—Diabetic wild-type mice showed a strong renal induction of type VIII collagen. Diabetic *Col8a1*$^{-}$/*Col8a2*$^{-}$ animals revealed reduced mesangial expansion and cellularity and extracellular matrix expansion compared with the wild type. These were associated with less albuminuria. High-glucose medium as well as various cytokines induced *Col8a1* in cultured mesangial cells. *Col8a1*$^{-}$/*Col8a2*$^{-}$ mesangial cells revealed decreased proliferation, less phosphorylation of Erk1/2, and increased $p27^{Kip1}$ expression. Overexpression of *Col8a1* in mesangial cells induced proliferation.

CONCLUSIONS—Lack of type VIII collagen confers renoprotection in diabetic nephropathy. One possible mechanism is that type VIII collagen permits and/or fosters mesangial cell proliferation in early diabetic nephropathy. ***Diabetes*** **58:1672–1681, 2009**

From the [1]Department of Medicine, University of Hamburg, Hamburg, Germany; the [2]Department of Pathology, University of Hamburg, Hamburg, Germany; the [3]Department of Medicine, Friedrich Schiller University, Jena, Germany; and the [4]Department of Developmental Biology, Harvard School of Dental Medicine, Boston, Massachusetts.

Corresponding author: Ulrike Hopfer, ulrike.hopfer@unibas.ch.

Received 10 February 2008 and accepted 6 April 2009.

Published ahead of print at http://diabetes.diabetesjournals.org on 28 April 2009. DOI: 10.2337/db08-0183.

U.H. and H.H. contributed equally to this study.

Diabetic nephropathy is the most common cause of end-stage renal failure leading to dialysis. Glomerular lesions are characterized by expansion of the mesangial matrix and thickening of peripheral glomerular basement membranes due to the synthesis and accumulation of extracellular matrix (ECM) (1,2). The degree of mesangial matrix expansion correlates with the progressive decline in the glomerular capillary surface area available for filtration and, hence, with the glomerular filtration rate (3). Early changes include a confined proliferation of mesangial cells followed by cell cycle arrest and hypertrophy (3–8). Several growth factors have been implicated in this process, among them transforming growth factor-β1 (TGF-β1) and platelet-derived growth factor (PDGF)-BB (4,9,10). During early stages, PDGF-BB potently increases proliferation and matrix synthesis of mesangial cells and induces the expression of TGF-β1 (4,5,11). Upregulation of the PDGF-BB pathway has been shown in kidneys from patients with diabetic nephropathy as well as in experimental models of diabetic nephropathy (12,13). Further, PDGF receptor antagonists attenuate diabetic nephropathy (4). Activation of the TGF-β1 loop leads to cell cycle arrest, induction of cyclin-dependent kinase inhibitors, and further ECM synthesis (3,14).

Type VIII collagen, a nonfibrillar short-chain collagen, is a structural component of many extracellular matrices (15–17). Two highly homologous polypeptides, α1(VIII) and α2(VIII), form either homotrimeric or heterotrimeric molecules (18–20). Type VIII collagen is involved in cross-talk between cells and the surrounding matrix by modulating diverse cellular responses such as proliferation, adhesion, migration, chemotaxis, and metalloproteinase synthesis (21–23). It is highly expressed by vascular smooth muscle cells in response to PDGF-BB and is thought to be a key component of vascular remodeling (24–27). In healthy kidneys, expression of type VIII collagen has been demonstrated in glomerular arterioles, larger branches of renal arteries, and in rat glomeruli and mesangial cell in vitro (28,29). Increased mRNA as well as protein expression has been noted in glomeruli and the tubulointerstitium of biopsies of kidneys from patients with diabetic nephropathy (30,31). The functional role of collagen VIII, especially in the early phase of the disease, has not been investigated and remains obscure.

To address the role of type VIII collagen in the pathogenesis of diabetic nephropathy, we applied the streptozotocin (STZ) model to mice with homozygous deletions of both collagen VIII genes and compared them with wild-type mice. The objectives of this study were to assess whether collagen VIII–dependent pathways are involved in the development of diabetic nephropathy and in various

TABLE 1
Variables measured during the study period of STZ-induced diabetes

	Body weight (g)		Blood glucose (mg/dl)	Urinary glucose (g/dl)	Albuminuria (OD/mm^2)
	Initial	End			
Col8a1$^{-/-}$/*Col8a2*$^{-/-}$ controls	24.6 ± 1.3	31.4 ± 1.8	128.5 ± 28.7	0	0.2 ± 0
Col8a1$^{-/-}$/*Col8a2*$^{-/-}$ STZ	27.2 ± 3.5	26.9 ± 3.3*	292.4 ± 66.6*	3.7 ± 0.9	0.3 ± 0.2*
Col8a1$^{+/+}$/*Col8a2*$^{+/+}$ controls	26.9 ± 2.3	29.7 ± 2.5	155.7 ± 36	0	0.1 ± 0.1
Col8a1$^{+/+}$/*Col8a2*$^{+/+}$ STZ	26.8 ± 3.4	26.2 ± 3.2†	319 ± 61.2†	3.8 ± 1	0.5 ± 0.3†‡

Data are means ± SD. *$P < 0.01$ vs. *Col8*$^{-/-}$ controls. †$P < 0.01$ vs. *Col8*$^{+/+}$ controls. ‡$P < 0.05$ vs. STZ *Col8*$^{-/-}$.

cellular and molecular processes associated with this disorder.

RESEARCH DESIGN AND METHODS

Animal experiments were approved by the local animal care committee of the University of Hamburg and done in accordance with the German Animal Protection Law. *Col8a1*$^{-}$/*Col8a2*$^{-}$ mice crossed for at least 20 generations into the C57BL/6 background (21) and wild-type mice were maintained in a pathogen-free facility. All animals had free access to water and were fed standard rodent chow. Systolic blood pressure was measured using tail cuff plethysmography (TSE Systems, Bad Homburg, Germany).

Disease model. Eight- to 10-week-old male mice were randomly divided into groups treated with STZ (Sigma, Deisenhofen, Germany) or left untreated. STZ was dissolved in sterile citrate buffer and injected intraperitoneally (150 mg/kg body weight) within 10 min of preparation on 3 consecutive days. To render animals hyperglycemic without becoming ketoacidotic, a subcutaneous insulin implant (LinShin, Toronto, ON, Canada) was administered. Fifteen *Col8a1*$^{-}$/*Col8a2*$^{-}$ mice and 12 wild-type mice were treated with STZ; 7 *Col8a1*$^{-}$/*Col8a2*$^{-}$ mice and 10 wild-type mice were left untreated. Urinary glucose levels (Diabur Test 5000; Roche, Mannheim, Germany) and body weight were examined at the beginning and the end of this study. Venous blood glucose concentrations were measured with a B-glucose analyzer (HemoCue, Ängelholm, Sweden). Urine samples were collected in metabolic cages at baseline and before sacrifice. Mice were killed after 40 days. Blood urea nitrogen (BUN) was measured by a multianalyzer (Hitachi, Ramsey, NJ).

Quantification of albuminuria. Two microliters of urine were placed in 18 μl of Laemmli buffer, boiled, and subjected to 12% SDS-PAGE. Gels were stained by Coomassie Blue following standard procedures, and pictures were taken of native gels. The albumin band with a molecular weight of 66.2 kDa was assessed densitometrically as described previously (32).

Histology, immunohistochemistry, and immunofluorescence. Kidneys were fixed in 10% buffered formalin, and 4-μm sections were stained with hematoxylin-eosin and periodic acid Schiff (PAS) reagent. For immunohistochemistry, paraffin sections were incubated with protease XXIV (15 min, 5 mg/ml), blocked with 5% normal horse or goat serum (30 min, room temperature), and incubated with anti-laminin (1:3,600, overnight, 4°C) or anti–collagen IV (1:600, overnight, 4°C) (both from Southern Biotechnology, Eching, Germany), followed by biotinylated donkey IgG (1:400, 30 min, room temperature). Signal amplification was performed with an ABC-AP kit (Vector Laboratories, Loerrach, Germany) according to the manufacturer's instructions using Neufuchsin as a substrate. For immunofluorescence, kidneys were fixed in 10% buffered formalin, infiltrated with 20% sucrose, and frozen in OCT. Cryosections (5 μm) were rehydrated, treated with proteinase XXIV, blocked in 5% goat serum in PBS, and incubated with rabbit anti–enhanced green fluorescent protein (EGFP) antibodies (1:500, 1 h, 37°C; Molecular Probes, Karlsruhe, Germany). A nonimmune rabbit serum was used as a control. Fluorescein anti-rabbit IgG was applied as a secondary antibody. For double immunofluorescence, staining with an anti-EGFP antibody was performed as above; the secondary antibody was a Texas Red anti-rabbit IgG. Sections were further incubated with anti-CD31/antiplatelet endothelial cell adhesion molecule-1 (PECAM-1) (1 h, room temperature; BD Biosciences, Franklin Lakes, NJ); the secondary antibody was a fluorescein anti-rat antibody.

Morphometric analysis. Twenty glomerular cross sections per mouse were photographed with an Axioscope microscope equipped with an Axiocam and evaluated with KS300.1 software (Zeiss, Oberkochen, Germany) in a double-blind fashion. The area of the glomerular cross section, the glomerular tuft, and the number of nuclei were measured. Results are expressed as percent glomerular tuft area and number of nuclei per glomerular cross section. Capillary density was measured by taking 20 pictures of each section stained against CD31 and evaluated with ImageJ64.

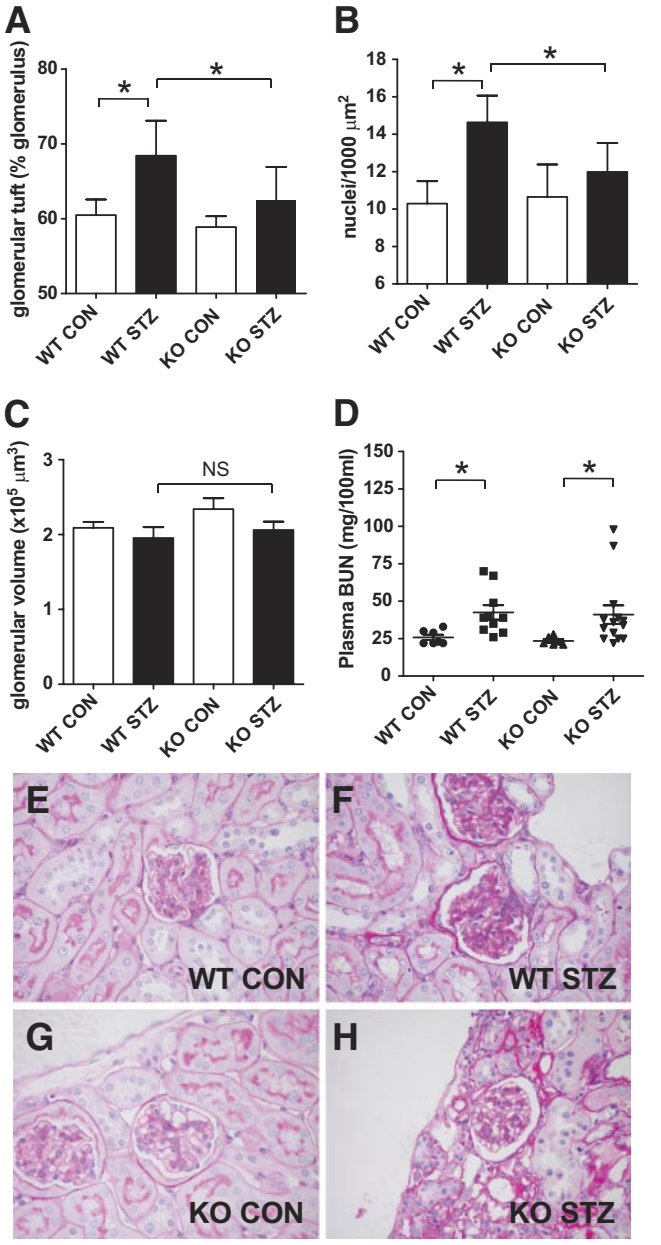

FIG. 1. Morphometry of diabetic (■) and nondiabetic (□) wild-type and *Col8a1*$^{-}$/*Col8a2*$^{-}$ *mice. A*: Mesangial tuft area per glomerulus (square millimeters). *B*: Mesangial nuclei per 1,000 μm^2. *C*: Glomerular volume. *D*: Plasma BUN (mg/100 ml). Bars represent SE; *$P < 0.05$, n = 10–12. Representative PAS stainings of nondiabetic wild-type (*E*) and *Col8a1*$^{-}$/*Col8a2*$^{-}$ *mice* (*G*) and diabetic wild-type (*F*) and *Col8a1*$^{-}$/*Col8a2*$^{-}$ *mice* (*H*). CON, control; KO, knockout; WT, wild-type. (A high-quality digital representation of this figure is available in the online issue.)

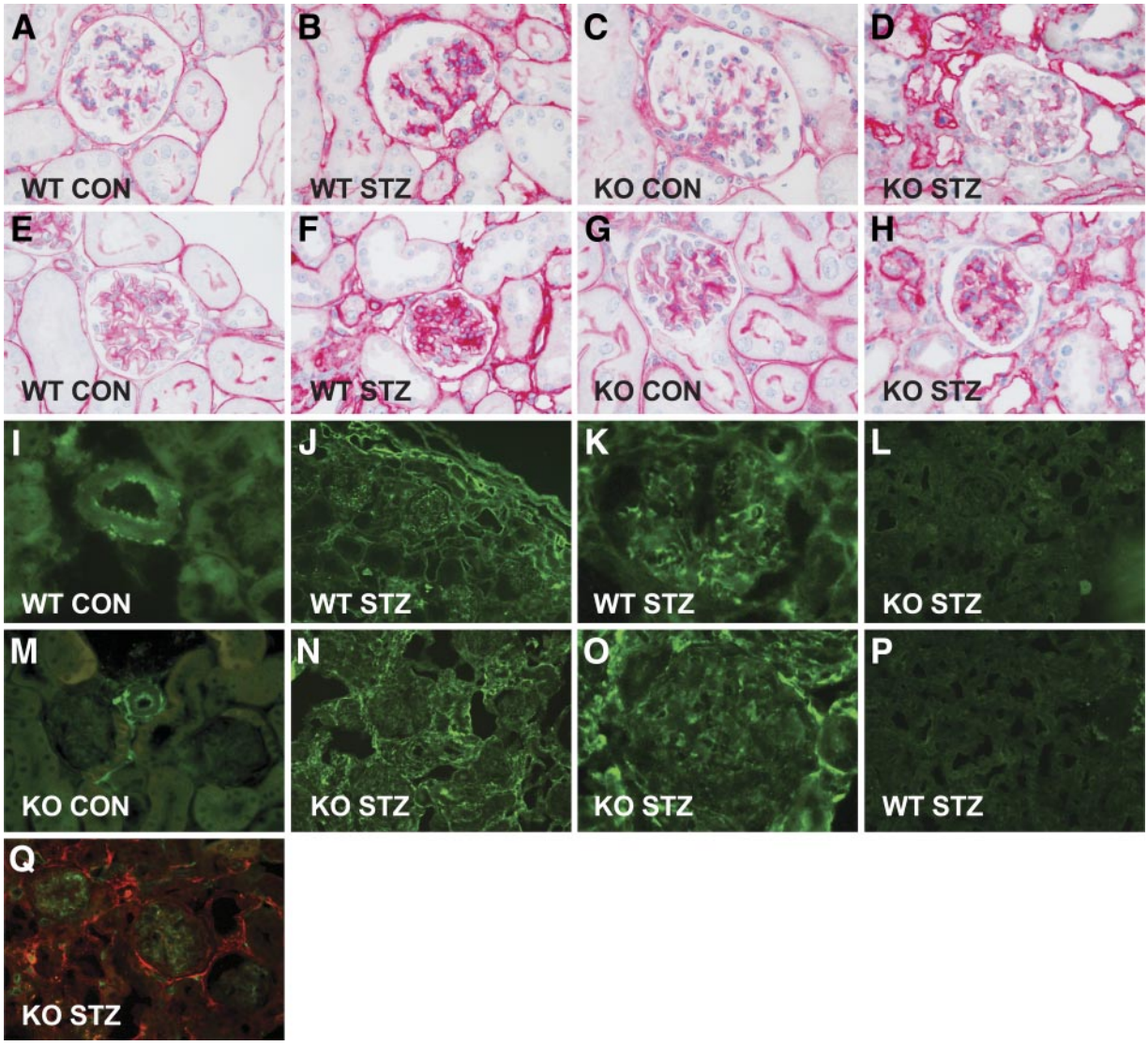

FIG. 2. Light microscopic features of the glomerular lesions and expression of type VIII collagen. Representative glomerulus of an untreated wild-type mouse (*A* and *E*) and a *Col8a1*$^{-}$*/Col8a2*$^{-}$ *mouse* (*C* and *G*) stained against type IV collagen (*A* and *C*) and laminin (*E* and *G*). Representative glomerulus of a wild-type mouse (*B* and *F*) and a *Col8a1*$^{-}$*/Col8a2*$^{-}$ *mouse* (*D* and *H*) treated with STZ and stained against type IV collagen (*B* and *D*) and laminin (*F* and *H*). Diabetes was associated with an increase in type IV collagen and laminin protein expression. Lack of collagen VIII reduced the accumulation of type IV collagen (*C* and *D*) and laminin (*G* and *H*) in the glomeruli. Immunofluorescence staining against collagen VIII in wild-type mice (*I, J,* and *K*) or EGFP in *Col8a1*$^{-}$/EGFP "knock-in" mice (*M, N,* and *O*). Strong staining for collagen VIII (*I*) and EGFP (*M*) was seen in healthy mice within the adventitia and the endothelium of arteries, whereas no staining was apparent in tubuli or glomeruli. In diabetic mice strong staining within the tubular interstitium, within the glomeruli, and around arterioles (anti–type VIII collagen [*J* and *K*] and anti-EGFP [*N* and *O*]). No staining against type VIII collagen was seen in *Col8a1*$^{-}$*/Col8a2*$^{-}$ *mice* (*L*) or EGFP in wild-type mice (*P*). Double immunofluorescence revealed that EGFP (red) only partly colocalized with CD31/PECAM-1 (green), a marker for vascular endothelial cells (*Q*). Original magnification: ×200 or ×400. CON, control; KO, knockout; WT, wild-type. (A high-quality digital representation of this figure is available in the online issue.)

Cell culture, transfection, and Western blot analysis and isolation of RNA and Northern blots. Detailed descriptions can be found in the supplemental data (available in an online appendix at http://care.diabetes journals.org/cgi/content/full/db08-0183/DC1).

Isolation and characterization of mouse mesangial cells. Two different isolates of wild-type and *Col8a1*$^{-}$*/Col8a2*$^{-}$ mouse mesangial cells (MMCs) were released from glomeruli using a modification of a published method (33). In brief, for each experiment two wild-type and two knockout mice were killed and immediately perfused with 8×10^7 Dynalbeads (Dynal, Invitrogen, Karlsruhe, Germany) diluted in 40 ml Hanks' balanced salt solution (HBSS) through the heart. Kidneys were removed, minced into 1-mm^3 pieces, and digested in 1 mg/ml collagenase A (Roche) and 100 units/ml DNase I in HBSS at 37°C for 30 min. The tissue was gently pressed through a 90-μm cell strainer and washed with 5 ml HBSS. The filtrate was passed though a new cell strainer without pressing and washed again. The cell suspension was then centrifuged at 200*g* for 5 min and resuspended in 2 ml HBSS. Finally, glomeruli containing Dynalbeads were gathered by a magnetic particle concentrator and washed three times with HBSS. Collagenase-digested glomeruli were seeded into cell culture dishes and maintained in Dulbecco's modified Eagle's medium, 10% serum and 1% glutamine, 100 units/ml penicillin, and 100 μg/ml streptomycin (Invitrogen) at 37°C and 5% CO_2 for 6 days. MMCs were passaged every 4–5 days.

For characterization, cells were grown on glass coverslips, fixed with 10% formalin, and photographed with a phase-contrast microscope or fixed with methanol (10 min on ice) for immunostaining. Cells were washed with PBS, blocked with 3% BSA in PBS (30 min, room temperature), and incubated with the primary antibodies (1 h, 37°C) and fluorescein-labeled anti-mouse-, anti-rat-, or anti-rabbit IgG (1:200, 1 h, 37°C). Primary antibodies were anti–collagen VIII (Seikagaku, Tokyo, Japan), anti-EGFP (Molecular Probes), anti-vimentin, anti-desmin, anti–smooth muscle actin (Sigma), anti-CD31/PECAM-1, and anti–collagen IV (ICN, Northeim, Germany). Isotype-matched IgG and nonimmune rabbit IgG were used as controls. Pictures were taken at ×200 magnification with an Axioscope fluorescence microscope.

Thymidine incorporation and growth curves. MMCs (passages 4–10) were plated on 96-well plates at a density of 3×10^3 cells/well and maintained in Dulbecco's modified Eagle's medium supplemented with 100 mg/dl glucose

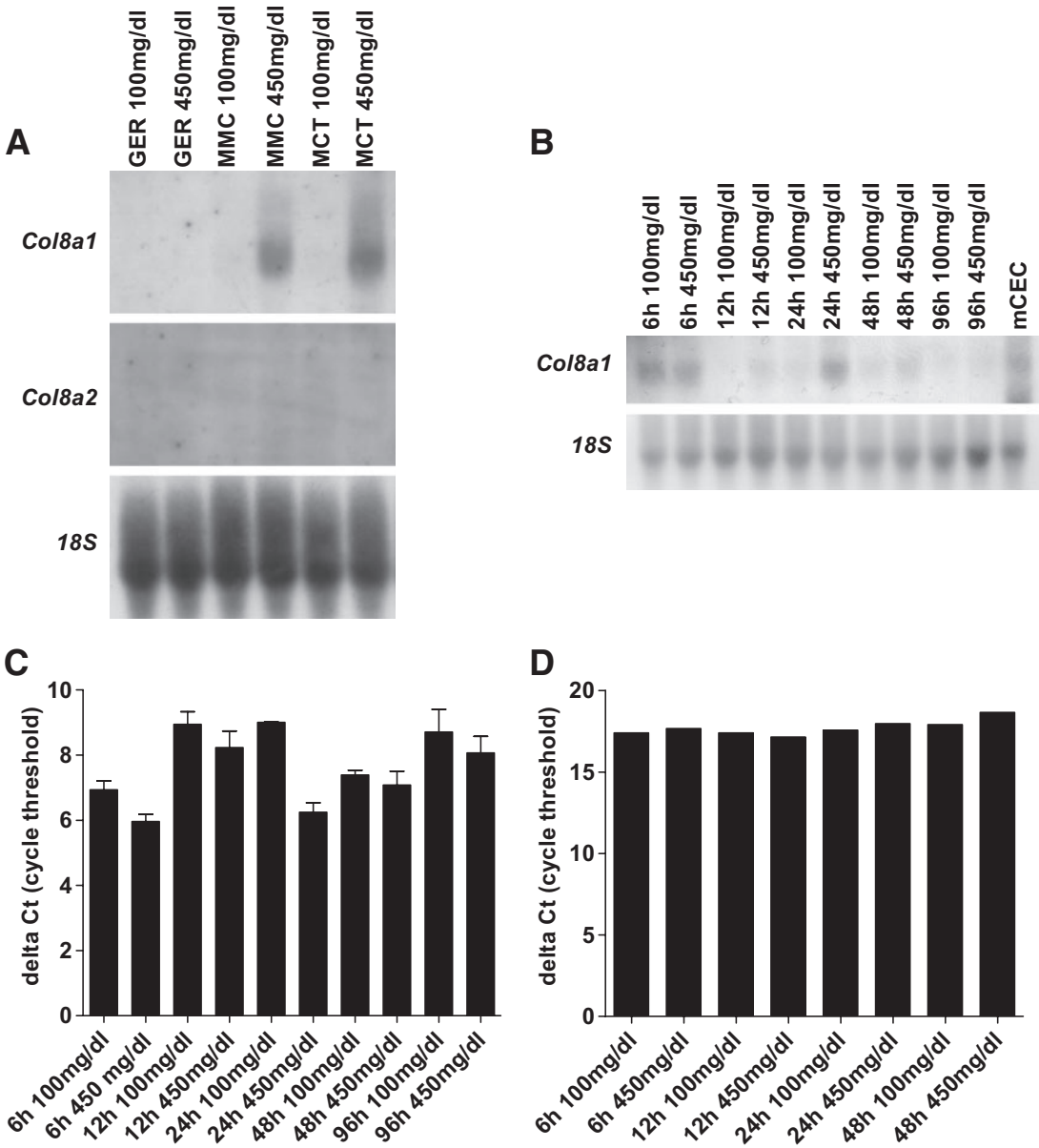

FIG. 3. High glucose induces *Col8a1*. *A*: Increased D-glucose concentrations (from 100 to 450 mg/dl) raised the *Col8a1* mRNA in tubular epithelial (MCT) and mesangial (MMC) cells but not in glomerular endothelial cells (GER) in Northern blots. *B*: High glucose increased the *Col8a1* mRNA expression in MMCs after 6 h. *C*: mRNA of murine corneal endothelial cell (mCEC) represent a positive control. *D*: Representative real-time PCR analyses on glucose-treated MMCs. Increased D-mannitose concentrations had no effect on the *Col8a1* expression.

and 10% FCS for 24 h to allow cell attachment. Serum-free medium was then added for 24 h to synchronize the cells in the G_0 phase. DNA synthesis was measured by [^{3}H]thymidine incorporation: 2 μCi/ml [^{3}H]thymidine was added for 16 h in the presence or absence of either 450 mg/dl glucose or 50 ng/ml PDGF-BB. Cells were washed twice with PBS, trypsinized, and harvested onto filter paper using an automated cell harvester (Dynatech Laboratories, Chantilly, VA). [^{3}H]thymidine incorporation was measured in a scintillation counter. Cell proliferation was further measured using the 3-(4,5-dimethylthiazol-2-yl)-2,5-diphenyltetrazolium assay (Roche Diagnostics). Results were plotted as means of 12 different values. Experiments were repeated three times with two different cell preparations. In a second set of experiments, MMCs (15×10^4) were seeded into six-well plates, stimulated as described above, trypsinized, and counted using a hemocytometer. D-Mannose (450 mg/dl) served as an osmotic control.

Quantitative real-time PCR. Rested MMCs were either stimulated with 25 ng/ml epidermal growth factor (EGF), basic fibroblast growth factor (bFGF), TGF-β1 (all from PeproTech, Hamburg, Germany), or PDGF-BB for 12, 24, and 48 h or treated as described for Northern blots. RNA was purified using a RNA extraction kit. For quantitative PCR amplifications of *Col8a1*, DNase I–treated first-strand cDNA was used with components of the SYBR Green JumpStart *Taq* Ready Mix (Sigma) on an AbiPrism NN8650 system. The cycling parameters were 50°C for 2 min and 95°C for 10 min, followed by 40 cycles of 95°C for 15 s and 60°C for 1 min. In each experiment, three or more identical PCRs of *Col8a1* and the control RNA *18S* were run using the primers for *18S* (sense 5′-CACGGCCGGTACAGTGAAAC-3′ and antisense 5′-AGAGGAGCGAGCGACCAAA-3′) and for *Col8a1* (sense 5′-TCTGCCACCTCAAATCCCTCCTCA-3′ and antisense 5′-TCTCCGCGCAAACTGGCTAACG-3′). The data were calculated by the comparative Ct method ($2-\Delta\Delta$Ct method), by which $\Delta\Delta$Ct = ΔCt sample − ΔCt reference. Threshold cycles were determined using the default threshold levels, and the average threshold cycles were normalized for amplification of *18S* as an internal control to correct for small variations in RNA quantity and cDNA synthesis. Relative expression levels were normalized to the unstimulated control. Melting curves and 3% NuSieve agarose gel electrophoresis were used to verify the absence of nonspecific PCR products. Three separate experiments were performed for each experiment, and one representative experiment is shown.

Statistical analysis. All data are presented as means ± SE. Statistical significance between multiple groups was tested with the Kruskal-Wallis test. Individual groups were subsequently tested using the Wilcoxon-Mann-Whitney test. $P < 0.05$ was considered significant. Experiments that did not yield enough independent data points for statistical analysis because of the

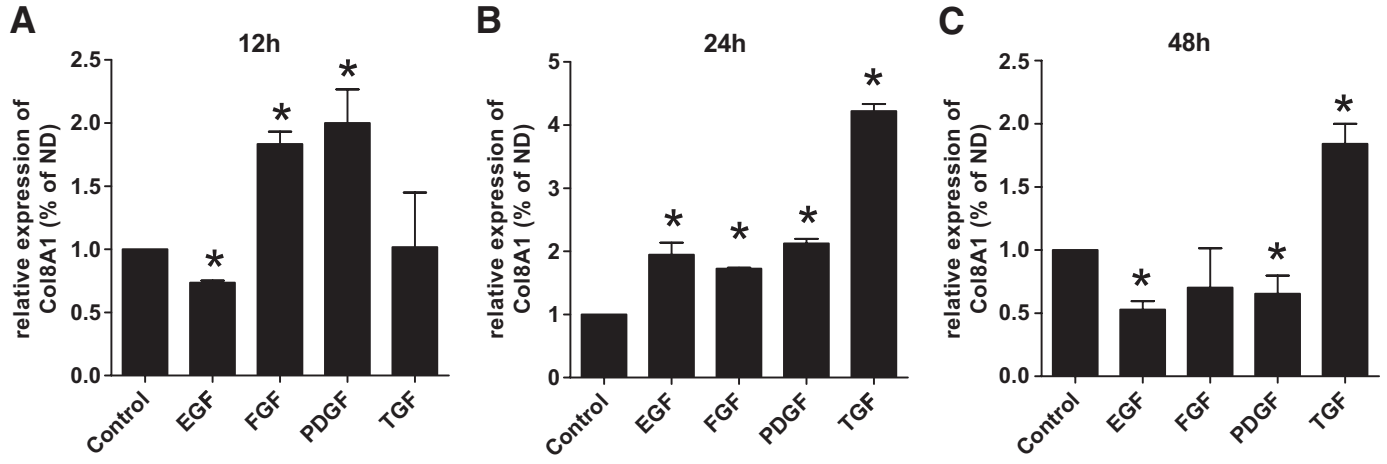

FIG. 4. Real-time PCR of *Col8a1* mRNA of MMCs in response to different cytokines. Wild-type MMCs were stimulated with 25 ng/ml EGF, bFGF, PDGF-BB, or TGF-β1 for 12, 24, and 48 h. After 12 h (*A*) strong *Col8a1* expression was seen by PDGF-BB and bFGF and none by TGF-β1 and EGF. TGF-β1 was the strongest inductor of *Col8a1* after 24 h followed by PDGF-BB, EGF, and bFGF (*B*). *C*: Stimulation for 48 h with TGF-β1 still had an effect on the *Col8a1* expression, but none by bFGF, EGF, and PDGF-BB. Bars represent SE; *$P < 0.05$.

experimental setup were repeated three times; one representative experiment is shown.

RESULTS

STZ-induced diabetes in wild-type and *Col8a1*$^{-}$/*Col8a2*$^{-}$ mice. Type VIII collagen was shown to be expressed by mesangial cells. We therefore hypothesized that lack of type VIII collagen may alter early mesangial changes seen in diabetic nephropathy. We induced diabetes by the short high-dose protocol of repeated STZ injections. Both wild-type and *Col8a1*$^{-}$/*Col8a2*$^{-}$ mice injected with STZ developed elevated levels of blood glucose as well as glucosuria. At the end of the study the diabetic wild-type and *Col8a1*$^{-}$/*Col8a2*$^{-}$ mice had failed to gain weight compared with the nondiabetic controls, but there was no significant difference between wild-type and knockout mice (Table 1 and data not shown). STZ-treated mice developed albuminuria. However, the albumin excretion of diabetic *Col8a1*$^{-}$/*Col8a2*$^{-}$ mice was significantly lower compared with that of the wild-type mice ($P < 0.05$) (Table 1). Plasma BUN increased significantly with diabetes ($P < 0.05$), but there was no significant difference between genotypes (Fig. 1*D*). Tail plethysmography revealed no significant difference ($P < 0.8$) in systolic blood pressure of untreated wild-type (100 ± 3.8 mmHg, $n = 5$) and *Col8a1*$^{-}$/*Col8a2*$^{-}$ mice (99.2 ± 5.8 mmHg, $n = 5$).

Reduced mesangial expansion and cellularity in *Col8a1*$^{-}$/*Col8a2*$^{-}$ mice. Histological analysis revealed the characteristic features of STZ-induced diabetic kidney lesions in the wild-type mice as described previously (34). Morphometric quantification of the glomerular tuft area in proportion to the total area of the glomerular cross section revealed a significant increase in diabetic wild-type mice (68.4 ± 4.7%) compared with nondiabetic controls (60.5 ± 2.0%, $P < 0.05$) (Fig. 1*A*). In contrast, diabetic *Col8a1*$^{-}$/*Col8a2*$^{-}$ mice (62.5 ± 4.3%) had no significant increase compared with nondiabetic *Col8a1*$^{-}$/*Col8a2*$^{-}$ animals (58.9 ± 1.5%). This finding was supported by increased immunohistochemical staining for type IV collagen (Fig. 2*A–D*) and laminin (Fig. 2*E–H*).

In addition, diabetic wild-type mice showed significant glomerular hypercellularity (14.6 ± 1.4 vs. 10.3 ± 1.2 nuclei/1,000 glomerular micrometers squared in nondiabetic wild-type mice, $P < 0.05$), whereas there was no difference in STZ *Col8a1*$^{-}$/*Col8a2*$^{-}$ mice (12 ± 1.6 vs. 10.7 ± 1.7 nuclei/1,000 glomerular μm^2) (Fig. 1*B*). Examples of PAS stainings are shown in Fig. 1*E–H*. No significant difference was observed in the glomerular volume (Fig. 1*C*). The interstitial capillary density showed no significant difference (CD31^{+} pixels: wild-type controls, 1.37 ± 0.45%; wild-type STZ treated, 1.37 ± 0.52%; knockout controls, 1.49 ± 0.51%; and knockout STZ treated, 1.46 ± 0.45; NS, $n = 10–12$ for each group).

Expression of type VIII collagen in glomeruli of STZ-treated wild-type mice. Type VIII collagen was detected by immunofluorescence in the mesangium, in the interstitium, and around blood vessels in diabetic wild-type mice, whereas staining in the control mice only was seen within the adventitia and the endothelium of arteries (Fig. 2*I–K*). As expected, no staining was detectable in *Col8a1*$^{-}$/*Col8a2*$^{-}$ mice (Fig. 2*L*). Because the knockout mice contain an EGFP gene driven by the *Col8a1* promotor, we also studied EGFP expression in STZ-treated and control *Col8a1*$^{-}$/*Col8a2*$^{-}$ mice. The distribution was comparable to that in the wild-type mice in both the STZ-treated and the control groups (Fig. 2*M–P*). EGFP did not colocalize with CD31/PECAM-1, indicating that type VIII collagen is not synthesized by glomerular endothelial cells (Fig. 2*Q*).

High glucose induces Col8a1 but not Col8a2 in mesangial and tubular epithelial cells. To further investigate potential mechanisms, we evaluated mRNA expression of *Col8a1* and *Col8a2* in mesangial cells (MMCs), glomerular endothelial cells, and tubular epithelial cells (MCTs) under high-glucose conditions. Northern blot analysis revealed an increase of *Col8a1* in MMCs and MCTs after 24 h, whereas *Col8a2* expression was not detectable (Fig. 3*A*). A time course experiment in MMCs showed that *Col8a1* mRNA expression under high-glucose conditions was already present at 6 h (Fig. 3*B* and *C*). A real-time PCR was performed to quantify this effect. *Col8a1* mRNA expression was raised after 6 h and peaked at 24 h. Increasing D-mannose concentrations to equiosmolar concentrations had no effect, indicating that the high-glucose effect is independent of the medium osmolarity (Fig. 3*D*).

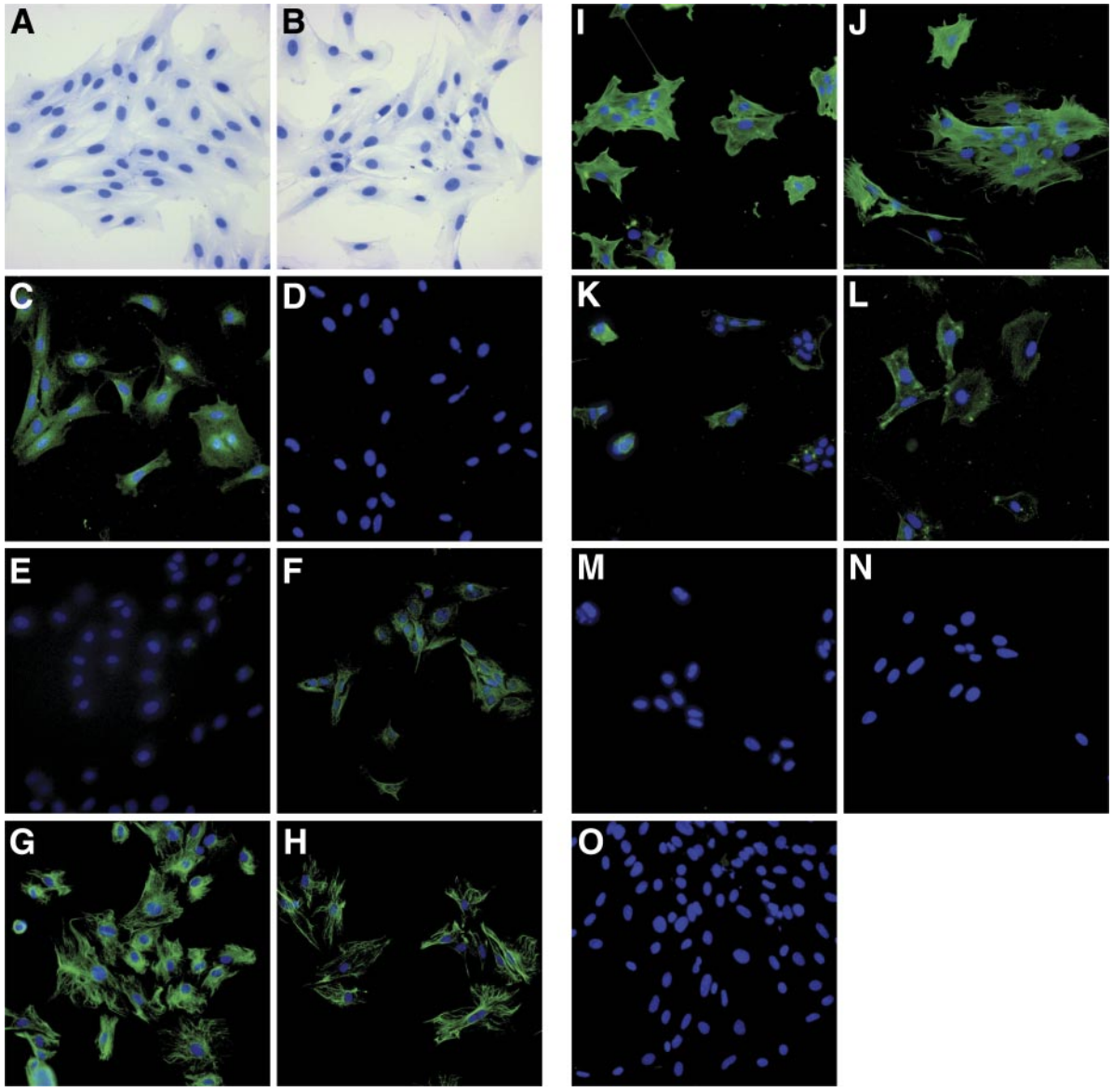

FIG. 5. Characterization of MMCs. The isolated mesangial cells showed the expected elongated stellate shape (*A* and *B*). An antibody against collagen VIII–stained wild-type (*C*) but not *Col8a1*$^{-}$/*Col8a2*$^{-}$ MMCs (*D*), whereas EGFP was stained in *Col8a1*$^{-}$/*Col8a2*$^{-}$ (*F*) but not wild-type MMCs (*E*). Intermediate filaments typical for MMCs stained positive: vimentin (*G* and *H*) and desmin (*K* and *L*). An antibody against cytoskeletal α–smooth muscle actin distinguished MMCs from fibroblasts (*I* and *J*). Staining MMCs with antibodies against markers specific for vascular endothelial cells such as CD31/PECAM-1 was negative (*M* and *N*). An isotype matched mouse IgG was used as control (*O*). Wild-type: *A, C, E, G, I, K, M,* and *O*; *Col8a1*$^{-}$/*Col8a2*$^{-}$: *B, D, F, H, J, L,* and *N*. Original magnification: ×200. (A high-quality digital representation of this figure is available in the online issue.)

PDGF-BB is an early regulator of *Col8a1* in MMCs. Because growth factors such as PDGF-BB and TGF-β1 (4,10) have been implicated in the pathogenesis of diabetic glomerulosclerosis, we determined the response of MMCs to different cytokines by real-time PCR. Wild-type MMCs were stimulated with EGF, bFGF, PDGF-BB, or TGF-β1 (Fig. 4). At 12 h, PDGF-BB (2.0 ± 0.4; $P < 0.05$) and bFGF (1.8 ± 0.1; $P < 0.05$) induced *Col8a1* ~2-fold, whereas there was no TGF-β1 (1.0 ± 0.6) or EGF effect (0.7 ± 0.0). At 24 and 48 h, TGF-β1 (24 h 4.2 ± 0.2, 48 h 1.8 ± 0.2; $P < 0.005$) was the strongest inductor. PDGF-BB and bFGF had a sustained effect at 24 h but not at 48 h. These results suggest that PDGF-BB and bFGF are early regulators of *Col8a1* expression, whereas TGF-β1 is more important at a later time point.

Decreased proliferation of *Col8a1*$^{-}$/*Col8a2*$^{-}$ MMCs. We isolated *Col8A1*$^{-}$/*Col8A2*$^{-}$ and wild-type MMCs to compare their ability to proliferate in response to glucose and PDGF-BB. Characterization of the primary mesangial cell cultures showed the expected elongated stellate shape in wild-type and *Col8a1*$^{-}$/*Col8a2*$^{-}$ mice (Fig. 5). By immunofluorescence, the cells stained positive for vimentin, desmin, and smooth muscle actin and were negative for CD31/PECAM-1. Wild-type MMCs were positive for type VIII collagen, whereas *Col8a1*$^{-}$/*Col8a2*$^{-}$ MMC stained for EGFP. [^{3}H]thymidine incorporation and cell counts were used as an index of MMC proliferation (Fig. 6*A* and *B*). High glucose stimulated cell proliferation significantly less in *Col8a1*$^{-}$/*Col8a2*$^{-}$ MMCs than in wild-type MMCs. Stimulation with PDGF-BB had an identical effect (Fig. 6*C* and *D*). D-Mannose had no impact on cell proliferation (Fig. 6*I*). Transfection of *Col8A1* into *Col8a1*$^{-}$/*Col8a2*$^{-}$ MMCs reversed the phenotype and prevented the decrease of proliferation in the *Col8a1*$^{-}$/*Col8a2*$^{-}$ cells after challenge with high glucose or PDGF-BB (Fig. 6*E–H*).

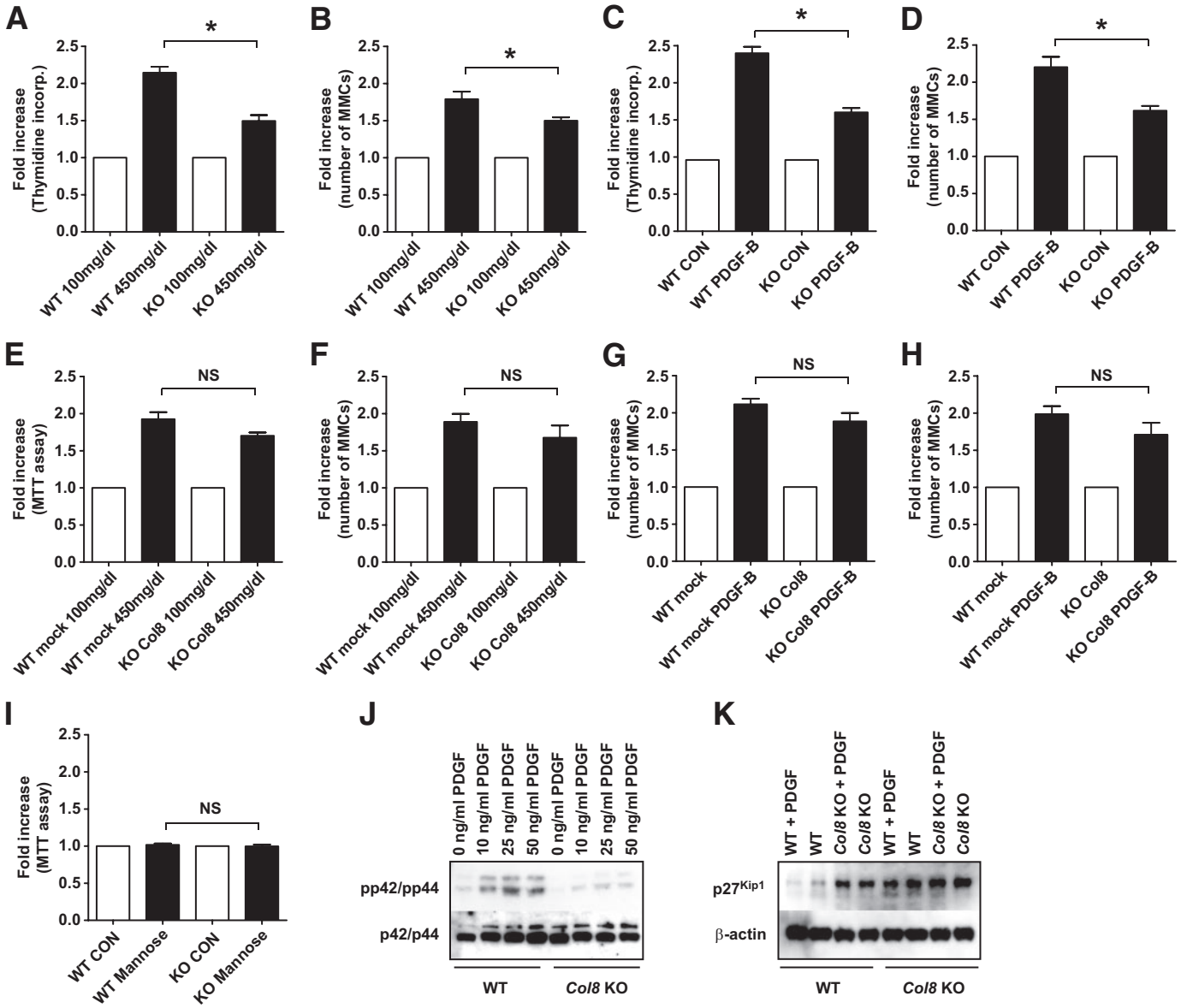

FIG. 6. Decreased proliferation of MMCs in *Col8a1*$^{-}$/*Col8a2*$^{-}$ MMCs. Thymidine incorporation by *Col8a1*$^{-}$/*Col8a2*$^{-}$ MMCs was significantly attenuated compared with that in wild-type controls (after glucose [*A*] and PDGF-BB stimulation [*C*]). Cell proliferation was also assessed by cell counts in the presence or absence of high glucose (*B*) or PDGF-BB (*D*). *E–H*: Transfection of *Col8A1* reversed the phenotype. *I*: Increased mannose concentrations had no impact upon proliferation. *J*: Further, compared with the wild type, *Col8a1*$^{-}$/*Col8a2*$^{-}$ cells had a lower pp42/pp44 level at the resting state and after stimulation with PDGF-BB in Western blots. *K*: p27^{Kip1} levels were increased in *Col8a1*$^{-}$/*Col8a2*$^{-}$ MMCs, and stimulation with PDGF-BB had no further effect. **P* < 0.01 vs. wild-type MMC. Bars represent SE. CON, control; KO, knockout; WT, wild-type.

The discoidin domain receptor tyrosine kinase (DDR1) functions as a collagen receptor on MMCs and signals by mitogen-activated protein kinase (MAPK) phosphorylation (35). Because *Col8a1*$^{-}$/*Col8a2*$^{-}$ MMCs proliferated at a slower pace than wild-type MMCs, we evaluated the amount of ERK1/2 (p42/p44) MAPK phosphorylation (Fig. 6*J*). Compared with wild-type cells, *Col8a1*$^{-}$/*Col8a2*$^{-}$ cells had a lower pp42/44 level in the resting state. Upon stimulation with PDGF-BB, *Col8a1*$^{-}$/*Col8a2*$^{-}$ MMCs showed markedly decreased p42/44 phosphorylation compared with wild-type MMCs.

Because increased proliferation is associated with a decrease in the cell cycle inhibitor p27^{Kip1} and MAPK directly phosphorylated and stabilized p27^{Kip1} (36), we investigated whether type VIII collagen also alters the expression of p27^{Kip1} (Fig. 6*K*). As predicted, PDGF-BB induced downregulation of p27^{Kip1} in wild-type MMCs. In contrast, the levels of p27^{Kip1} were increased in *Col8a1*$^{-}$/*Col8a2*$^{-}$ MMCs, and stimulation with PDGF-BB had no further effect.

Overexpression of *Col8a1* leads to increased proliferation of MMCs. An MMC cell line overexpressing *Col8a1* was generated. A 2.5 ± 0.2-fold mRNA overexpression was determined by real-time PCR (data not shown). Stimulation with high glucose or PDGF-BB for 24 h resulted in a significant increase in thymidine incorporation and cell counts compared with those in mock-transfected cells (Fig. 7*A–D*). A mild induction of p42/44 was found, which was enhanced on stimulation with PDGF-BB (Fig. 7*E*).

DISCUSSION

Mesangial cells are a major player in the maintenance of glomerular integrity. This is accomplished in part through

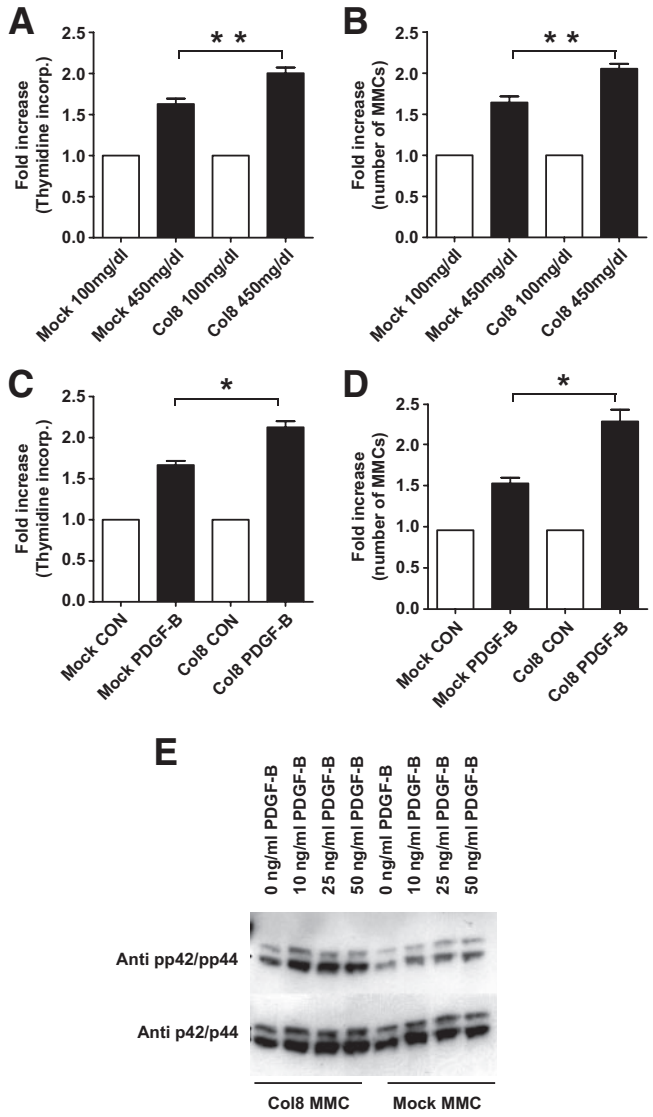

FIG. 7. Overexpression of *Col8a1* increased proliferation of MMCs. Stimulation with glucose (*A*) or 50 ng/ml PDGF-BB (*C*) for 24 h leads to an increase in thymidine incorporation of *Col8a1* MMCs compared with mock-transfected MMCs. Cell counts confirmed increased growth of *Col8a1* MMCs compared with mock-transfected cells (stimulation with glucose [*B*] or PDGF-BB [*D*]). Bars represent SE. *$P < 0.05$; **$P < 0.01$. Western blots stained with the phosphorylation specific p42/p44 antibody revealed an induction of p42/p44 in *Col8a1* MMCs, which was low in mock-transfected MMCs (*E*). CON, control; KO, knockout; WT, wild-type.

expression of ECM proteins and growth factors. In diabetic glomerulosclerosis, elevated glucose results in pronounced alterations of mesangial cell function with an early limited proliferation of mesangial cells (4–8), followed by cell cycle arrest, hypertrophy (3), excess production, and decreased degradation of ECM components including collagens, fibronectin, laminin, and proteoglycans (37). These multiple steps are orchestrated by growth factors and hormones (10,12).

Several features of type VIII collagen suggest that it could play an important role in mesangial cell function and the pathogenesis of diabetic glomerulosclerosis. It is part of the mesangial matrix in diabetic nephropathy (30,31), mesangial cells synthesize α1(VIII) collagen (16,29), and type VIII collagen has been shown to modulate cell proliferation of diverse cells including vascular smooth muscle cells (23,27,38). We used genetically modified mice deficient in both *Col8* genes to test its role in diabetic nephropathy in the STZ model (21). Several principal findings emerged from our study: *1*) in the absence of type VIII collagen the severity of the glomerular changes is markedly attenuated and albuminuria is improved, *2*) high glucose, PDGF-BB, and TGF-β1 are strong inducers of *Col8a1* gene expression in MMCs, and *3*) α1(VIII) collagen permits and/or stimulates MMC proliferation.

Our in vivo data clearly show that type VIII collagen is necessary for mesangial matrix expansion as well as for hypercellularity. Type VIII collagen accumulated in the mesangium of diabetic wild-type mice. This finding is consistent with previous reports of human kidney biopsies (30,31). Our in vitro data help to explain this difference. High glucose increases *Col8a1* mRNA expression by mesangial cells, whereas *Col8a2* mRNA was not detectable. This result suggests the formation of α1(VIII) collagen homotrimers in the diabetic mesangium. Growth factors such as PDGF-BB, bFGF, and TGF-β1 have been implicated in the pathogenesis of diabetic glomerulosclerosis (4,9), and the expression of *Col8a1* in vascular smooth muscle cells has been described after stimulation with these factors (25,26). Therefore, it is not surprising that PDGF-BB and bFGF act as early regulators of *Col8a1* expression in MMCs followed by TGF-β1. This kinetic effect parallels the early activation of a PDGF loop that, in turn, causes an increase in TGF-β1 expression, thus modulating both mesangial cell proliferation and matrix production (11,39). Induction of diabetic nephropathy is associated with increased proliferation of mesangial cells, and treatment of diabetic mice with antagonists for the PDGF receptor reduced the number of proliferating cells (4). MMCs with inactivated *Col8a1* and *Col8a2* genes proliferate less in response to high glucose or growth factors than wild-type MMCs. In addition, overexpression of α1(VIII) collagen results in increased cell growth. Type VIII collagen is expressed by a number of rapidly proliferating cells, and it promotes vascular smooth muscle cell migration and proliferation during vascular remodeling (21–24,27). Therefore, pericellular type VIII collagen may help maintain the mesangial cells in a proliferative state during early development of diabetic nephropathy. This hypothesis is consistent with the finding that *Col8a1*$^{-}$/*Col8a2*$^{-}$ vascular smooth muscle cells exhibited lower proliferation rates than wild-type cells when plated on type I collagen (27), thus suggesting that endogenously produced type VIII collagen allows smooth muscle cells to overcome the inhibitory effects of type I collagen on proliferation, which may also be important in the context of diabetic nephropathy.

Because systolic blood pressure was not significantly different in wild-type and *Col8a1*$^{-}$/*Col8a2*$^{-}$ mice and no significant change in interstitial capillary density was observed, we think that the change in the mesangium phenotype is the major mechanism explaining the attenuation of diabetic nephropathy in *Col8a1*$^{-}$/*Col8a2*$^{-}$ mice.

Over the last few years toxicity has become a major concern in the STZ model of diabetes (34). STZ has a dose-dependent tubular toxicity, resulting in renal dysfunction and acute tubular necrosis (40). Therefore, studies of renal function and tubulointestinal changes should be interpreted with caution because it is difficult to dissect the contribution of hyperglycemia and toxicity, especially in high-dose protocols as used in our study. However, to our knowledge, there is no evidence that the diffuse

glomerulosclerosis in the STZ model can also be attributed to a toxic side effect of SZT. In humans, STZ does not cause diabetes (41) and is used to treat metastatic islet cell carcinomas of the pancreas. Although renal tubulotoxicity is the major dose-limiting side effect of this drug (42), there have been no reports of diffuse or nodular glomerulosclerosis in >25 years in clinical use. In mice, several studies comparing low- and high-dose protocols showed a similar degree of diffuse glomerulosclerosis in both groups (34,43). In addition, blood glucose control by insulin treatment of rats rendered diabetic with STZ prevented diffuse glomerulosclerosis (44).

MAPKs, including ERK1/2 (p42/p44), play a key role in the intracellular signal transduction cascade to integrate the transcription of genes responsible for a variety of cellular responses relevant to diabetic nephropathy (45). Our data indicate a role of type VIII collagen in activating ERK1/2. This activation may be achieved through the collagen receptor DDR1, which is a key regulator of mesangial cell proliferation and is stimulated by type VIII collagen (35,46). Whereas the unstimulated receptor suppresses ERK1/2 activation, the activated DDR1 induces ERK1/2 phosphorylation and subsequent proliferation. Mesangial cell proliferation is governed at the level of the cell cycle by regulatory proteins. Specifically, cyclin-dependent kinase inhibitors including $p27^{Kip1}$ limit cell proliferation by binding to and inhibiting cyclin-cyclin–dependent kinase complexes (47). Consistent with decreased proliferation in *Col8a1*$^{-}$/*Col8a2*$^{-}$ MMCs, the levels of $p27^{Kip1}$ were increased compared with those in wild-type mice.

In summary, we provided evidence that type VIII collagen acts as an important messenger molecule regulating mesangial cell responses during diabetic nephropathy. The lack of type VIII collagen confers renoprotection in the STZ model of diabetic nephropathy. We concluded that type VIII collagen may function to permit and/or foster mesangial cell proliferation in the early stage of diabetic nephropathy.

ACKNOWLEDGMENTS

This work was supported by a grant from the Deutsche Forschungsgemeinschaft to G.W. (WO460, 14-1).

No potential conflicts of interest relevant to this article were reported.

Parts of this study were presented as a poster at the annual meeting of the American Society of Nephrology, San Diego, California, 14–19 November 2006 (J Am Soc Nephrol 2006;17:632A–633A).

We acknowledge Regine Schröder and Katarina Jablonski for excellent technical assistance, Ulrich Wenzel for blood pressure measurements, and Gunter Zahner for helpful discussions.

REFERENCES

1. Wolf G, Chen S, Ziyadeh FN. From the periphery of the glomerular capillary wall toward the center of disease: podocyte injury comes of age in diabetic nephropathy. Diabetes 2005;54:1626–1634
2. Mason RM, Wahab NA. Extracellular matrix metabolism in diabetic nephropathy. J Am Soc Nephrol 2003;14:1358–1373
3. Wolf G. Molecular mechanisms of diabetic mesangial cell hypertrophy: a proliferation of novel factors. J Am Soc Nephrol 2002;13:2611–2613
4. Lassila M, Jandeleit-Dahm K, Seah KK, Smith CM, Calkin AC, Allen TJ, Cooper ME. Imatinib attenuates diabetic nephropathy in apolipoprotein E-knockout mice. J Am Soc Nephrol 2005;16:363–373
5. Young BA, Johnson RJ, Alpers CE, Eng E, Gordon K, Floege J, Couser WG, Seidel K. Cellular events in the evolution of experimental diabetic nephropathy. Kidney Int 1995;47:935–944
6. Wolf G, Sharma K, Chen Y, Ericksen M, Ziyadeh FN. High glucose-induced proliferation in mesangial cells is reversed by autocrine TGF-β. Kidney Int 1992;42:647–656
7. Nabokov A, Waldherr R, Ritz E. Demonstration of the proliferation marker Ki-67 in renal biopsies: correlation to clinical findings. Am J Kidney Dis 1997;30:87–97
8. Horney MJ, Shirley DW, Kurtz DT, Rosenzweig SA. Elevated glucose increases mesangial cell sensitivity to insulin-like growth factor I. Am J Physiol 1998;274:F1045–F1053
9. Nakamura T, Fukui M, Ebihara I, Osada S, Nagaoka I, Tomino Y, Koide H. mRNA expression of growth factors in glomeruli from diabetic rats. Diabetes 1993;42:450–456
10. Ziyadeh FN, Hoffman BB, Han DC, Iglesias-De La Cruz MC, Hong SW, Isono M, Chen S, McGowan TA, Sharma K. Long-term prevention of renal insufficiency, excess matrix gene expression, and glomerular mesangial matrix expansion by treatment with monoclonal antitransforming growth factor-β antibody in *db/db* diabetic mice. Proc Natl Acad Sci USA 2000;97:8015–8020
11. Di Paolo S, Gesualdo L, Ranieri E, Grandaliano G, Schena FP. High glucose concentration induces the overexpression of transforming growth factor-β through the activation of a platelet-derived growth factor loop in human mesangial cells. Am J Pathol 1996;149:2095–2106
12. Kelly DJ, Gilbert RE, Cox AJ, Soulis T, Jerums G, Cooper ME. Aminoguanidine ameliorates overexpression of prosclerotic growth factors and collagen deposition in experimental diabetic nephropathy. J Am Soc Nephrol 2001;12:2098–2107
13. Langham RG, Kelly DJ, Maguire J, Dowling JP, Gilbert RE, Thomson NM. Over-expression of platelet-derived growth factor in human diabetic nephropathy. Nephrol Dial Transplant 2003;18:1392–1396
14. Wolf G, Ziyadeh FN. Molecular mechanisms of diabetic renal hypertrophy. Kidney Int 1999;56:393–405
15. Muragaki Y, Shiota C, Inoue M, Ooshima A, Olsen BR, Ninomiya Y. alpha 1(VIII)-collagen gene transcripts encode a short-chain collagen polypeptide and are expressed by various epithelial, endothelial and mesenchymal cells in newborn mouse tissues. Eur J Biochem 1992;207:895–902
16. Kittelberger R, Davis PF, Flynn DW, Greenhill NS. Distribution of type VIII collagen in tissues: an immunohistochemical study. Connect Tissue Res 1990;24:303–318
17. Sawada H, Konomi H, Hirosawa K. Characterization of the collagen in the hexagonal lattice of Descemet's membrane: its relation to type VIII collagen. J Cell Biol 1990;110:219–227
18. Illidge C, Kielty C, Shuttleworth A. The α1(VIII) and α2(VIII) chains of type VIII collagen can form stable homotrimeric molecules. J Biol Chem 1998;273:22091–22095
19. Stephan S, Sherratt MJ, Hodson N, Shuttleworth CA, Kielty CM. Expression and supramolecular assembly of recombinant α1(viii) and α2(viii) collagen homotrimers. J Biol Chem 2004;279:21469–21477
20. Illidge C, Kielty C, Shuttleworth A. Type VIII collagen: heterotrimeric chain association. Int J Biochem Cell Biol 2001;33:521–529
21. Hopfer U, Fukai N, Hopfer H, Wolf G, Joyce N, Li E, Olsen BR. Targeted disruption of *Col8a1* and *Col8a2* genes in mice leads to anterior segment abnormalities in the eye. FASEB J 2005;19:1232–1244
22. Iruela-Arispe ML, Diglio CA, Sage EH. Modulation of extracellular matrix proteins by endothelial cells undergoing angiogenesis in vitro. Arterioscler Thromb 1991;11:805–815
23. Hirano S, Yonezawa T, Hasegawa H, Hattori S, Greenhill NS, Davis PF, Sage EH, Ninomiya Y. Astrocytes express type VIII collagen during the repair process of brain cold injury. Biochem Biophys Res Commun 2004;317:437–443
24. Bendeck MP, Regenass S, Tom WD, Giachelli CM, Schwartz SM, Hart C, Reidy MA. Differential expression of α_1 type VIII collagen in injured platelet-derived growth factor-BB-stimulated rat carotid arteries. Circ Res 1996;79:524–531
25. Sibinga NE, Foster LC, Hsieh CM, Perrella MA, Lee WS, Endege WO, Sage EH, Lee ME, Haber E. Collagen VIII is expressed by vascular smooth muscle cells in response to vascular injury. Circ Res 1997;80:532–541
26. Hou G, Mulholland D, Gronska MA, Bendeck MP. Type VIII collagen stimulates smooth muscle cell migration and matrix metalloproteinase synthesis after arterial injury. Am J Pathol 2000;156:467–476
27. Adiguzel E, Hou G, Mulholland D, Hopfer U, Fukai N, Olsen B, Bendeck M. Migration and growth are attenuated in vascular smooth muscle cells with type VIII collagen-null alleles. Arterioscler Thromb Vasc Biol 2006;26:56–61
28. Kittelberger R, Davis PF, Greenhill NS. Immunolocalization of type VIII collagen in vascular tissue. Biochem Biophys Res Commun 1989;159:414–419

29. Rosenblum ND, Briscoe DM, Karnovsky MJ, Olsen BR. α_1-VIII collagen is expressed in the rat glomerulus and in resident glomerular cells. Am J Physiol 1993;264:F1003–F1010
30. Gerth J, Cohen CD, Hopfer U, Lindenmeyer MT, Sommer M, Grone HJ, Wolf G. Collagen type VIII expression in human diabetic nephropathy. Eur J Clin Invest 2007;37:767–773
31. Ruger BM, Hasan Q, Greenhill NS, Davis PF, Dunbar PR, Neale TJ. Mast cells and type VIII collagen in human diabetic nephropathy. Diabetologia 1996;39:1215–1222
32. Eremina V, Sood M, Haigh J, Nagy A, Lajoie G, Ferrara N, Gerber HP, Kikkawa Y, Miner JH, Quaggin SE. Glomerular-specific alterations of VEGF-A expression lead to distinct congenital and acquired renal diseases. J Clin Invest 2003;111:707–716
33. Takemoto M, Asker N, Gerhardt H, Lundkvist A, Johansson BR, Saito Y, Betsholtz C. A new method for large scale isolation of kidney glomeruli from mice. Am J Pathol 2002;161:799–805
34. Tay YC, Wang Y, Kairaitis L, Rangan GK, Zhang C, Harris DC. Can murine diabetic nephropathy be separated from superimposed acute renal failure? Kidney Int 2005;68:391–398
35. Curat CA, Vogel WF. Discoidin domain receptor 1 controls growth and adhesion of mesangial cells. J Am Soc Nephrol 2002;13:2648–2656
36. Wolf G, Reinking R, Zahner G, Stahl RA, Shankland SJ. Erk 1,2 phosphorylates $p27^{Kip1}$: Functional evidence for a role in high glucose-induced hypertrophy of mesangial cells. Diabetologia 2003;46:1090–1099
37. Phillips A, Janssen U, Floege J. Progression of diabetic nephropathy. Insights from cell culture studies and animal models. Kidney Blood Press Res 1999;22:81–97
38. Iruela-Arispe ML, Hasselaar P, Sage H. Differential expression of extracellular proteins is correlated with angiogenesis in vitro. Lab Invest 1991;64: 174–186
39. Fraser D, Wakefield L, Phillips A. Independent regulation of transforming growth factor-β1 transcription and translation by glucose and platelet-derived growth factor. Am J Pathol 2002;161:1039–1049
40. Levine BS, Henry MC, Port CD, Rosen E. Toxicologic evaluation of streptozotocin (NSC85998) in mice, dogs and monkeys. Drug Chem Toxicol 1980;3:201–212
41. Yang H, Wright Jr. Human β cells are exceedingly resistant to streptozotocin in vivo. *Endocrinology* 143:2491–2495,2002
42. Weiss RB: Streptozocin: a review of its pharmacology, efficacy, and toxicity. Cancer Treat Reports 1982;66:427–438
43. Inada A, Kanamori H, Arai H, Akashi T, Araki M, Weir GC, Fukatsu A. A model for diabetic nephropathy: advantages of the inducible cAMP early repressor transgenic mouse over the streptozotocin-induced diabetic mouse. J Cell Physiol 2008;215:383–291
44. Rasch R, Dorup J. Quantitative morphology of the rat kidney during diabetes mellitus and insulin treatment. Diabetologia 1997;40:802–809
45. Haneda M, Koya D, Isono M, Kikkawa R. Overview of glucose signaling in mesangial cells in diabetic nephropathy. J Am Soc Nephrol 2003;14:1374–1382
46. Hou G, Vogel W, Bendeck MP. The discoidin domain receptor tyrosine kinase DDR1 in arterial wound repair. J Clin Invest 2001;107:727–735
47. Wolf G, Schroeder R, Thaiss F, Ziyadeh FN, Helmchen U, Stahl RA. Glomerular expression of p27Kip1 in diabetic *db/db* mouse: role of hyperglycemia. Kidney Int 1998;53:869–879